

## POLYMER FLAT LOOP THERMOSYPHONS

**Grakovich L.P., Rabetsky M.I., Vasiliev L.L., Vasiliev L.L., Jr.**

Luikov Heat and Mass Transfer Institute, National Academy of Sciences of Belarus, P. Brovka 15, 220072,  
Minsk, Belarus

E-mail: [leonard\\_vasiliev@rambler.ru](mailto:leonard_vasiliev@rambler.ru)

**Bogdanovich S.P., Pesetskii S.S.**

V.A. Belyi Metal Polymer Research Institute of National Academy of Sciences of Belarus, Kirov St. 32A,  
246050 Gomel, Belarus

### ABSTRACT

Heat dissipation necessity becomes an extremely important issue for electronics production, air-conditioning, LED cooling systems and refrigeration. The technology was developed to produce new loop polymer thermosyphons capable of long-term operation without permeation by air or working fluids through their walls. Suggested composite polymer materials with high thermal conductivity are employed as the case material and give possibilities to design a wide range of new heat transfer equipment. In this paper the flat horizontal polymer loop thermosyphon with flexible transport lines is suggested and experimentally tested. Its evaporator and condenser are reinforced with nano carbon filaments and nano particles to improve its thermal conductivity, durability and wettability. The rectangular capillary grooves inside the evaporator and condenser are used as a mean for the heat transfer enhancement. The working fluid is R 600. Thin film evaporation heat transfer for low heat load and two phase flow (vapor bubbles and liquid slugs) heat transfer for high heat load inside the evaporator are inherent for such thermosyphon.

**KEY WORDS:** heat pipe, loop thermosyphon, polymer composite, nano particles, evaporator, condenser, flexible transport lines, thermal resistance.

The present topic of the paper is related to the field of cooling technologies for air-conditioning, refrigeration, LED cooling systems and electronics package and is based on the innovative means for thermal energy handling at better operating conditions in comparison to traditional technologies. Actually polymer heat transfer equipment is used in different devices [Guan-Wei Wu et al., 2012; Masataka Mochizuki et al., 2013; Vasiliev 2013]. Polymer-metal composites are becoming an attractive subject due to their unique surface morphology, Carlberg B, Ye LL, Liu J: 2012. They can be made on the base of polymeric films metalized from one, or both sides with a noble metal (gold or platinum), Kim KJ, Shahinpoor M., 2003; Slepíčka P. et al., 2012. Considerable efforts have been devoted to the design and fabrication of controlled organic/inorganic composites with novel properties, including optical, electrical, chemical, biological, and mechanical properties, Bledzki AK, Gassa, 1999; Stankovich S, Dikin DA, et al. 2006. In these hybrid systems, phase separation occurs naturally because they are composed of two materials with totally different chemical characteristics, Lipatov YS, Nesterov AE, et al. 2002. Besides the polymer-metal composites the

carbon fibre reinforced carbon composites, epoxy and phenolformaldehyde composites reinforced by glass and carbon wires, polyamide composite materials with nano carbon filaments and nano particles are also the subject of interest in the designing of the polymer loop thermosyphons and heat pipes, Bogdanovich et al., 2011. The envelope of such heat pipes have the effective thermal conductivity 10-40 times more to compare with the pure polymer material. The evaporator and condenser flat interface of such thermosyphons and heat pipes are interesting to be used for cooling the heat-generating elements and transfer the heat load to the heat sink. Actually some polymer heat transfer components are used in different devices, Guan-Wei Wu, Sih-Li Chen, Wen-Pin Shih, 2012; Masataka Mochizuki, Aliakbar Akbarzadeh and Thang Nguyen ,2013; L. L. Vasiliev and L. L. Vasiliev Jr., 2013.

In this work the polymer loop thermosyphon with flat interface (for heat-generating elements attachment) and flexible transport lines is presented. The thermosyphon passively transfers heat from a heat source to a heat sink where heat is dissipated. The thermosyphon has rectangular capillary grooves as the capillary structure inside the evaporator and condenser, Fig. 1(a-b). Its

frame, Fig. 1b, is made from the polyamide composite with nano carbon filaments and nano particles to increase its effective thermal conductivity up to 11 W/m °C, Bogdanovich et al.,2011. A jacket of polymer composite is formed around a core of carbon fibers to form a highly thermally conductive heat transfer device. The width and length of thermosyphon are 50 mm and 250 mm, respectively. The width of the grooved surface inside the evaporator and condenser, where two phase heat transfer occurs is 30 mm. The width and depth of the rectangular mini grooves inside the evaporator and condenser are 2.5 mm. The thickness of the evaporator and condenser is 10 mm. There are flexible vapor and liquid transport pipes (200 mm length, 5 mm diameter respectively) made from pure polyamide to connect the evaporator and condenser, which are disposed in parallel one below the other.



Figure 1a. Flat loop thermosyphon made from polymer composite.



Figure 1b. Flat evaporator (cross section view) with rectangular mini-channels.

The width and thickness of rectangular side parts of frames are 10 mm respectively. The working fluid of thermosyphon is isobutene (R 600). The experimental techniques was used to perform some necessary operations including temperature measurements (Agilent Data Acquisition Agilent Data Logger HP-34970A with a set of

thermocouples connected with computer), the measurement of the heat flow from the evaporator to condenser and effective thermal conductivity of the thermosyphon envelope. The experimental set-up, Fig.2, with the temperature sensors points on the evaporator, condenser, vapor and liquid pipes of thermosyphon was used during experiments. The heat flow enters the bottom side of the evaporator. The heat sink is on the top side of the condenser. The temperature difference  $T_w - T_{sat}$  between the external walls of the evaporator,  $T_w$ , and the saturated temperature of the adiabatic (vapor transport) zone,  $T_{sat}$ , was measured directly by four thermocouples, one junction of which was on the evaporator wall, while the other was placed in a thermally controlled liquid bath.

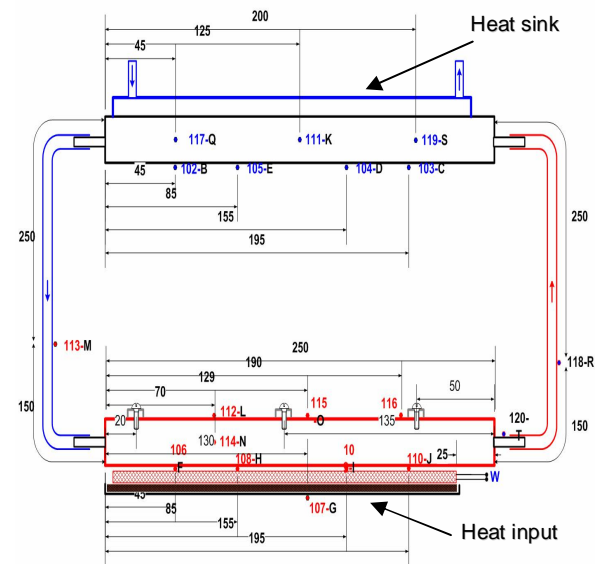


Fig. 2 Experimental set-up with thermocouples attachment in the evaporator, condenser and transport zone (vapor and liquid).

The vapor saturation inside the thermosyphon was maintained by regulation of temperature and fluid flow on the condenser heat sink (liquid heat exchanger).

The total thermosyphon thermal resistance,  $R_{ts}$ , was calculated as:

$$R_{ts} = (T_e - T_c) / W, \quad (1)$$

Where  $T_e$  (°C) - the mean evaporator temperature;  $T_c$  (°C) - the mean condenser temperature, and  $W$ (Watts) - the input power.

To cool the thermosyphon condenser (liquid loop) a Joulabo F12 recirculation thermal bath with temperature-regulated accuracy of  $\pm 0.5^\circ\text{C}$  was used. Heat flow was supplied by the electric

cartridge heater, disposed on the bottom surface of the evaporator. The heat sink (liquid heat exchanger) was attached to the top of the condenser. All measurements were performed in a steady-state regime for the heat flux range of 50–100 W.

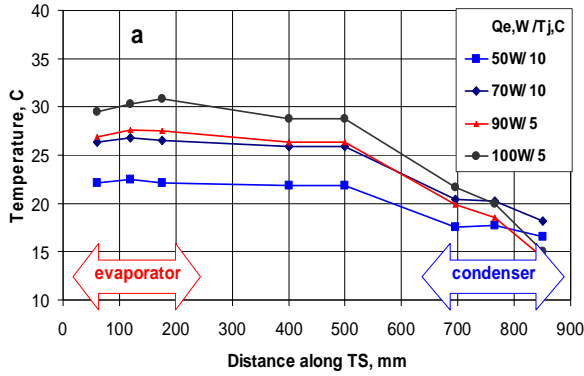


Fig. 3a Mean temperature distribution along the evaporator and condenser **top surface** of thermosyphon as the function of heat input  $W$ .

The temperature distribution along the evaporator, transport zone and condenser as a function of the heat load is shown on Fig. 3 (a, b).

The mean temperature profiles on the top surface of the evaporator and condenser are shown on Fig.3a, while the temperature profiles on the bottom surface of the evaporator and condenser are shown on Fig.3b. The temperature of saturated vapor inside the thermosyphon was varied from 20–40 °C with the help of thermostat thermal control.

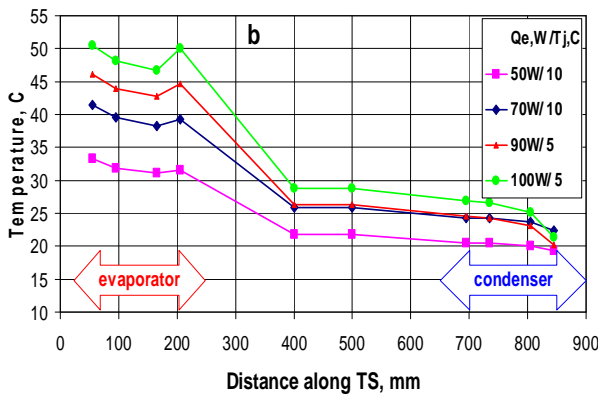


Figure 3b. Mean temperature distribution along the evaporator and condenser **bottom surface** of thermosyphon as the function of heat input,  $W$ .

Thermal resistances of evaporator and condenser as a function of heat input are shown in Fig. 4(a,b).

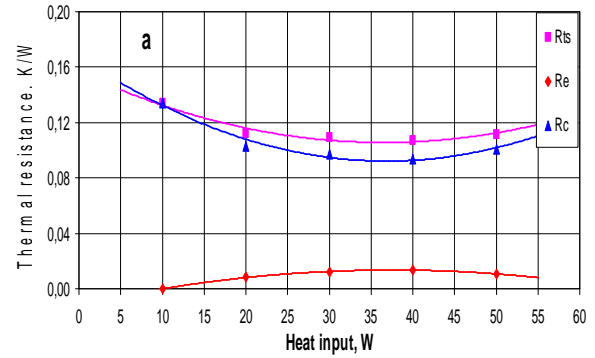


Figure 4a. Thermal resistance of evaporator ( $R_e$ ), condenser ( $R_c$ ) and total thermosyphon ( $R_{ts}$ ) as a function of the heat input (**top surface**).

Three zones of temperature distribution could be observed in the evaporator, transport zone (vapor line) and condenser. The temperature difference  $T_w - T_{sat}$  between the wall of the evaporator  $T_w$  and the saturated temperature of the vapor channel,  $T_{sat}$ , was measured directly by thermocouples.

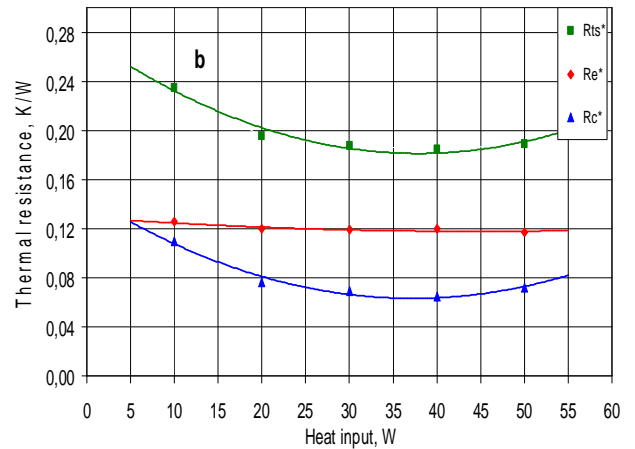


Figure 4b. Thermal resistance of evaporator ( $R_e^*$ ), condenser ( $R_c^*$ ) and total thermosyphon ( $R_{ts}^*$ ) as a function of the heat load (**bottom surface**).

Mean temperature distribution along the **bottom surface** of thermosyphon was used for  $R$  calculations, Fig. 4b. For this case  $R_{ts}$  is nearly two times more to compare with top surface measurements, Fig. 4a.

The difference of temperature between the top, bottom and side surfaces of the evaporator and condenser are shown on Fig. 5.

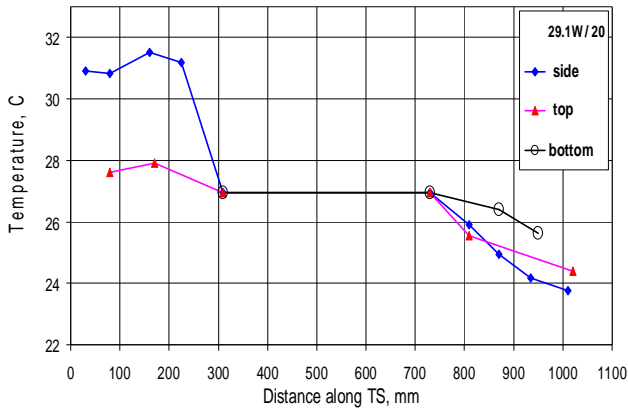


Figure 5 Mean temperature distribution along the side, top and bottom surfaces of evaporator, transport zone and condenser. Heat input is 29 W. Thermosyphon inclination to the horizontal axis is **2 degree**.

The mean temperature of the flank side of thermosyphon slightly differs from the mean temperature of the top and bottom due to the low heat transfer in this local part of thermosyphon, Fig. 5.

It is important to note, that thermosyphon is sensible to the mass of the working fluid charged, Fig.6. The mass of R 600 (13 g) was chosen just to fill the volume of capillary channels in the evaporator, condenser and liquid transport pipe at the room temperature, for the heat load 40 W.

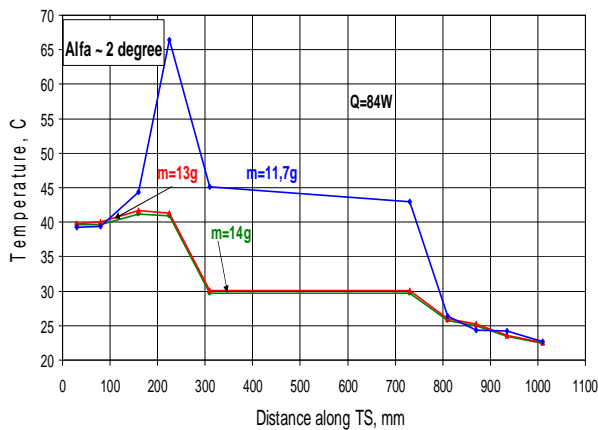


Figure 6. Mean temperature distribution along the surface of evaporator, vapor zone and condenser as a function of R 600 mass. Heat input is 84 W.

The analysis of the mean temperature distribution, Fig.6, along the thermosyphon for different mass of the working fluid denotes the change of total thermal resistance as a function of fluid mass, charged in thermosyphon. For the mass of R 600 equal 13g the total thermal resistance is optimal while the decreasing of mass down to 11.7 g

significantly increases the thermal resistance of the evaporator and is not sufficient to ensure the wettability of total heat loaded surface.

Increasing the mass of R 600 up to 14 g does not significantly changes the temperature distribution along the thermosyphon.

It is important to note, that the tilt of thermosyphon to the horizontal axis is not so critical, Fig.5 and Fig.7.

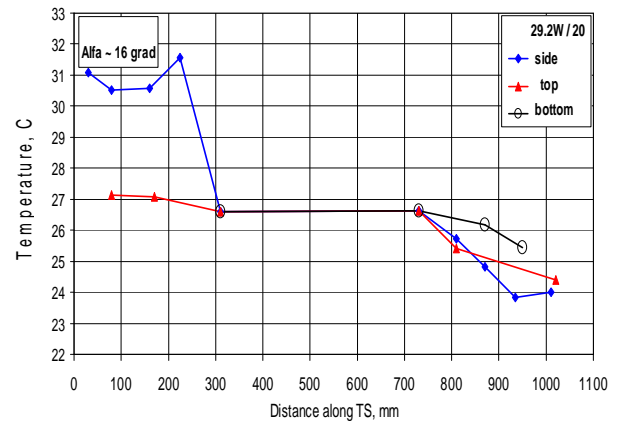


Figure 7. Mean temperature distribution along the thermosyphon, heat input is 29 W. The degree of the inclination to the horizontal axis is **16 degree**

The design of such thermosyphon guarantees a weak influence of the evaporator inclination to the horizontal axis in the limit of 0-20 degrees.

The difference between the temperature distribution in Fig. 5 and Fig. 7 is negligible.

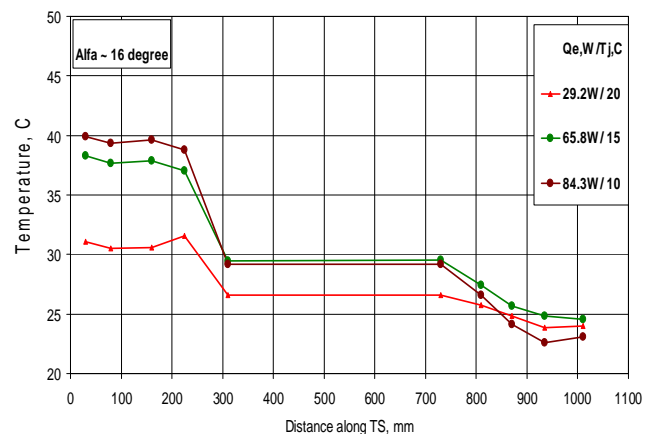


Figure 8. Mean temperature distribution along the thermosyphon as a function of heat input. The degree of thermosyphon inclination to the horizontal axis is **16 degree**.

## 6. RESULTS AND DISCUSSION

The set of preliminary experiments with new type of polymer loop thermosyphon show the possibility to apply such heat transfer devices as low temperature cooling technology. Recently developed a new polymer composite with increased thermal conductivity can be suggested as the thermosyphon envelope compatible with alcohol (methanol), water and some hydrocarbons (R 600) as a working fluid. Nanocoating of the heat loaded surface of such polymer have a grand potential to increase the wettability and heat transfer intensity in small size heat transfer devices, Vasiliev L.L. et al., 2012. Nano coating stimulates the bubble generation in mini-channels beginning of the certain heat load. Therefore investigation of evaporation, boiling and condensation heat transfer in mini-gchannels is a good tool to analyze the cooling efficiency of thermosyphon. Analyzing the data on Fig.4a and Fig.4b it is clear, that the thermal resistance of the evaporator  $R_e$  and condenser  $R_c$  strongly depend on the heat load and heat sink disposition in space. For the case, when the heat source is in the bottom of the evaporator, the evaporator thermal resistance  $R_e$  is much lower the  $R_c$ , Fig.4a. For the case, when the heat source is located on the top of the evaporator, its thermal resistance  $R_e$  is higher that  $R_c$ , Fig.4b. The mentioned above polymer thermosyphon configuration is offered only by an illustrative way, being possible detail modifications, especially as to shape, size and disposition of the parts. An object of this research is to provide a prototype of polymer thermosyphon, that is easily formable into a wide array of configurations.

The thermosyphon advantages are:

1. A first advantage is given from the fact that different prototypes of thermosyphon can be made of different polymer and loaded with additive or filler different from that loaded in the polymers of other capillary pipes, depending on the need

A second advantage is given from the fact that each capillary pipe can have suitable dimensions and shape as for example coil or zigzag

A further advantage is given from the fact that, unlike a traditional heat pipe, the interior of a pulsating heat pipe does not comprise a layer of porous material to pump the fluid into the evaporator zone by capillarity

This work shows a promising combination of technologies that has the potential to usher in a new generation of highly flexible, lightweight,

low-cost, high-performance thermal management solutions

## 7. CONCLUSIONS

The present design of thermosyphon relates to cooling of heat generating objects by use of composite materials.

1. New type of horizontal polymer flat loop thermosyphon with nanotechnology application was suggested, designed and tested with the thermal resistance value varying with the input heat flux and the tilt angle. The working fluid is R 600.

2. It was found that the grooved evaporator thermal resistance  $R_e$  of polymer thermosyphon is similar to that of classical aluminum smooth grooved heat pipe.

3. Horizontal thermosyphon is sensible to the mass of the working fluid charge. Slight undercharge increases the temperature of the evaporator and total thermal resistance.

4. The degree of the inclination of thermosyphon to the horizontal axis (up to 20 degree) only slightly increases the thermosyphon thermal resistance.

5. The combination of R 600, polymer (polyamide) and composite material (polyamide reinforced with nano carbon filaments and nano particles) as thermosyphon envelope is completely compatible. During 6 months of experiments with thermosyphon non-condensable gas generation inside the thermosyphon was not detected.

## REFERENCES

Bledzki AK, Gassan J: Composites reinforced with cellulose based fibres. *Prog Polym Sci* 1999, 24:221.

Bogdanovich S.P., Grakovich L.P., Vasiliev L.L. Heat-conductive polymerous material on basis of thermoelastolayers. Int. Conf. «Polymeric composite materials and tribology» (Polycomtrib-2011). Gomel, Belarus, (2011).

Carlberg B, Ye LL, Liu J: Polymer-metal nanofibrous composite for thermal management of microsystems. *Mater Lett* 2012, 75:229–232.

Christopher Oshman, Bo Shi, Chen Li, Ronggui Yang, Y. C. Lee, G. P. Peterson,

Victor M. Bright, "The Development of Polymer-Based Flat Heat Pipes", IEEE/ASME Journal of Microelectromechanical Systems, - J. MICROELECTRO MECHANICAL SYST, vol. 20, no. 2, pp. 410-417, (2011) DOI: 10.1109/JMEMS.2011.2107885

Guan-Wei Wu, Sih-Li Chen, Wen-Pin Shih, Lamination and characterization of a polyethylterephthalate flexible micro heat pipe, *Frontiers in Heat Pipes (FHP)*, 3, 023003 (2012)  
DOI: 10.5098/fhp.v3.2.3003, Available at [www.ThermalFluidsCentral.org](http://www.ThermalFluidsCentral.org)

Kim KJ, Shahinpoor M: Ionic polymer–metal composites: II. Manufacturing techniques. *Smart Mater Struct* 2003, 12:65–79.

Lipatov YS, Nesterov AE, Ignatova TD, Nesterov DA: Effect of polymer–filler surface interactions on the phase separation in polymer blends. *Polymer* 2002, 43:875.

Masataka Mochizuki, Aliakbar Akbarzadeh and Thang Nguyen , A Review of Heat Pipe Practical Applications and Innovative Opportunities Application for Global Warming, Heat Pipes and Solid Sorption Transformation: Fundamentals and Practical Applications , Mechanical, Aerospace & Nuclear Engineering. Taylor & Francis/CRC Press, USA, Editors: Leonard L. Vasiliev and Sadik Kakaç, (2013), 145-212

Slepička P, Fidler T, Vasina A, Švorčík V: Ripple-like structure on PLLA induced by gold deposition and thermal treatment. *Mater Lett* 2012, 79:4–6.

Stankovich S, Dikin DA, Dommett GHB, Kohlhaas KM, Zimney EJ, Stach EA, Piner RD, Nguyen ST, Ruoff RS: Graphene-based composite materials. *Nature* 2006, 442:282.

Vasiliev L.L., Grakovich L.P., Rabetsky M.I., Vasiliev L.L. Jr., (2012) Grooved heat pipes evaporators with porous coating,

Proceedings of the 16<sup>th</sup> IHPC, Lion, France, May 20-24.

Vasiliev L.L. and Vasiliev L.L. Jr. Heat Pipes and Thermosyphons for Solid Sorption Machines and Fuel Cells Thermal Management, Heat Pipes and Solid Sorption Transformation: Fundamentals and Practical Applications , Mechanical, Aerospace & Nuclear Engineering. Taylor & Francis/CRC Press, USA, Editors: Leonard L. Vasiliev and Sadik Kakaç, (2013), 259-282.

[Vasiliev Leonid Jr.](#), US Patent Heat exchange device made of polymeric material [US20110067843](#),